

Monitoring of River Morphological Change Using Remote Sensing and Hec-Ras in Lusi River, Indonesia

Diva Darma Wijaya¹, Jazaul Ikhsan¹, Nursetiawan^{1*}

¹ *Master of Civil Engineering, Postgraduate Program,
Universitas Muhammadiyah Yogyakarta, Bantul, Yogyakarta, 55183, INDONESIA*

*Corresponding Author: nursetiawan@umy.ac.id

DOI: <https://doi.org/10.30880/ijie.2024.16.05.038>

Article Info

Received: 20 December 2023

Accepted: 20 August 2024

Available online: 29 August 2024

Keywords

Erosion, remote sensing, river morphology, river flow change, hec-ras

Abstract

Changes in river flow have become a natural cycle of the river. The Lusi River has problems with meanders due to sediment transport, which is difficult to control. A combination of GIS with RS and HEC-RAS simulation was used to monitor river flow. The water monitoring method utilizes four water indices: NDWI, MNDWI, ANDWI, and SAVI, while the MPM-Toffaleti method is used for simulation. By combining the four methods, accuracy values of 0.68 to 0.92 and precision levels of 0.60 to 0.93 were obtained. MNDWI obtained quite high results compared to other indices. The results showed that the Lusi River experienced quite extreme flow changes. Two flow cuts occurred. Considerable erosion occurred from 2003 to 2013 with a total lost area of 0.1943 km², while from 2013 to 2023, there was erosion of 0.1177 km². The HEC-RAS simulation of the Lusi River experienced erosion of 60 to 70.4 percent of the length of the stream. Changes in the riverbed in 2013 were found to be -1.1 ± 2.03 m, and then in 2023, the range of changes in the riverbed was -2.69 ± 1.29 m. Based on the results of the index and simulation of the Lusi River experiencing erosion in the flow, the level of erosion has increased every period.

1. Introduction

Rivers are a natural resource that humans utilize. The natural activity of the river has a very dynamic system [1]. All activities that require the river's role will affect the shape of the flow [2]. Such as agricultural activities, farming, settlement, water distribution, sediment movement [3], and hydrological cycle [4]. Moreover, the evolution of river morphology results in changes in river flow [5]. Sediment transport has a high contribution. The height of sediment movement is influenced by grain gradation, grain weight, ambient temperature, flow discharge, and topology [6].

The Indonesian river system is characterized by a high degree of variability in flow patterns. It is a consequence of the geography of river flow. For example, the Lusi River exhibits a dry flow pattern. A similar flow pattern is observed in rivers situated in the northern region of Java Island. The similarity of the pattern is caused by the downstream region having a high concentration of volcanic deposits [7], as evidenced by the muddy coloration of the water in rivers with a high volcanic deposit load. The erosion of fine-grained river morphology conditions is a relatively rapid process. Climatic factors also play a role in changing river flow conditions [8], [9]. Furthermore, human activities that utilize river flows can also impact changes in flow patterns [9].

Following the development of technology, the Geographic Information System (GIS) has been used to control or monitor natural areas [10]. In this case, GIS is used to analyze satellite data to analyze river areas. Remote Sensing (RS) refers to the acquisition of data from a distance that projects images of the Earth [11]. So, performing a combination in this way can provide a clear image of the Earth. The United States Geological Survey (USGS) has developed Landsat satellites to observe the Earth's surface. Multispectral remote sensing can be used for the

automatic identification of water bodies [12] while monitoring geographical changes in rivers [13]. Data quality is greatly affected by the atmosphere and land cover, which distort the image pixels.

Monitoring the changing river morphology has been done, but only from one perspective. Additional simulations were performed using Hec-RAS to get another perspective on the changes. Monitoring of river erosion patterns using the results of Landsat satellite aerial observations from 2003 to 2023. The analysis was performed using indices derived from band combinations. Each index is compared and then validated with the results of the Hec-RAS sediment movement simulation.

2. Method

2.1. Study Area

This study is located in the Lusi River in Purwodadi district, Central Java province, Indonesia, which is shown in Fig. 1. The focus of the study was on the ± 21 km long mid-river area. The Lusi River itself is part of the Jragung, Tuntang, Serang, Lusi, Juana (Jratunseluna) river basin. The Jratunseluna area is a collection of 69 streams passing through 8 districts, with an area of 2093.1 km².

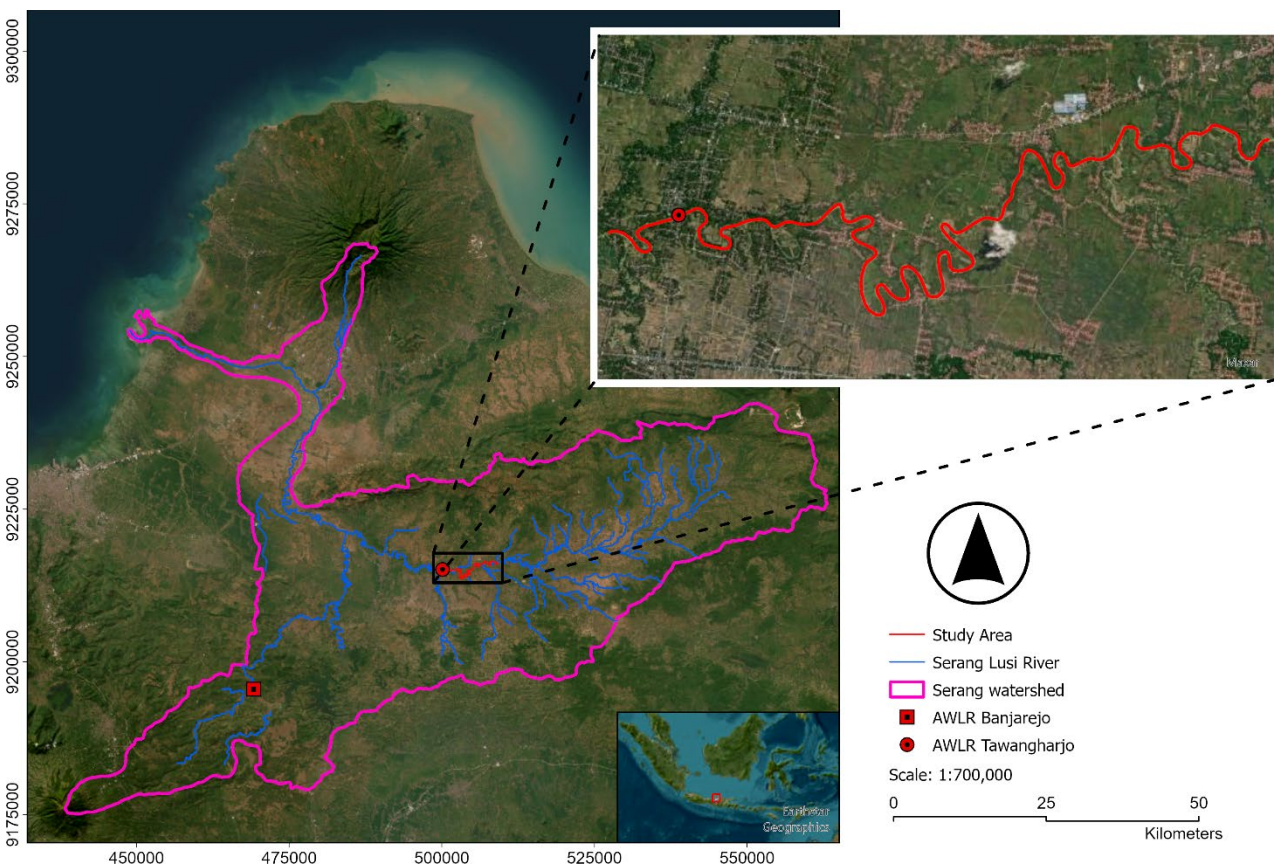


Fig. 1 Lusi Basin and River Segments

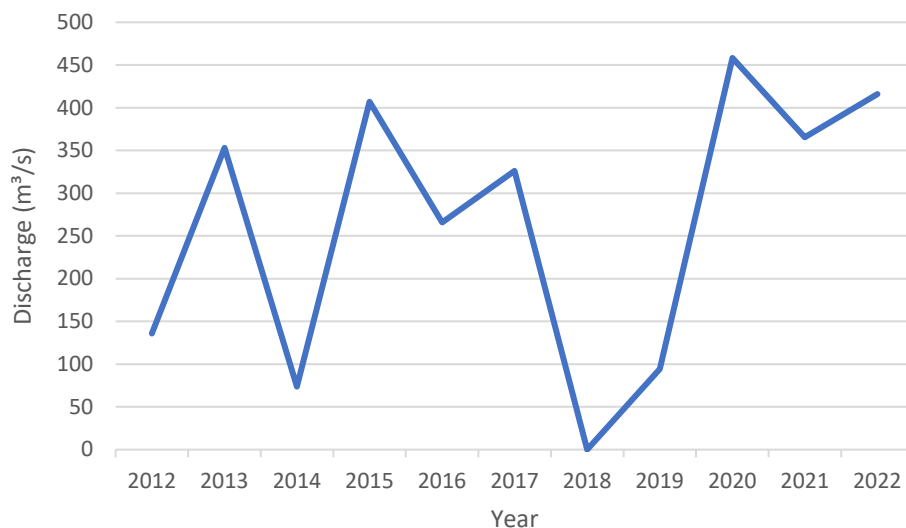
2.2. Data Collection

Satellite data collection utilized the data obtained from the Landsat satellite. The data captured in 2003, 2013, and 2023 are presented in Table 1. In analyzing the satellite imagery used, it is necessary to consider the limitations of the data set. While the original data set is comprised of images captured in the same year, with different months, the use of satellite data from the same year but different months allows for the representation of a situation that is not too different. Within 20 years, there are three different types of Landsat satellites, each with different capture capabilities influenced by the sensor technology used. Landsat 7 satellite uses Enhanced Thematic Mapper Plus (ETM+) technology with up to 8-bit image sharpness. It also has the disadvantage of processing data in one path, which causes a distance between image pixels. Then, in Landsat 8, the problem was fixed with Operational Land Imager (OLI) technology. The sharpness of the captured image has increased to 12-bit. For Landsat 9, there is an increase in image sharpness to 14-bit.

Table 1 Satellite data source details

Satellite	Day	Month	Year	Cloud Cover (%)	Path/Row	Source
Landsat-7	13	May	2003	13.00		
Landsat-8	9	September	2013	6.25	119/065	USGS
Landsat-9	12	January	2023	22.28		

The recorded discharge was obtained from the Tawangharjo AWLR downstream of the study area. Fig. 2 shows the highest discharge within ten years. In 2022, the highest discharge of 416 m³/s occurred in December, but in 2012, it occurred in May with 312 m³/s. Global climate change greatly affects river flow conditions. The impact is that the rain cycle in Indonesia becomes unpredictable and changes rapidly. The Lusi River is located at an altitude of 15 to 30 m above sea level. This condition makes the river flow carry volcanic material that settles. The soil characteristics are dominated by mud and sand [14]. Sediment transport consists of sand and mud, causing the river's color to tend to be cloudy due to mixing with mud, which can affect satellite band data.

**Fig. 2** Maximum monthly river discharge in a year

Flow simulation requires cross-sectional data to provide flow limits. In this research, simulations will be conducted in 2013 and 2023, which have a long time difference. So, we directly used cross-section data from 2013 conducted by the government. While the data in 2023 uses the Data Elevation Model (DEM) provided by the government. DEM data collection for Central Java Province was collected in 2018. The DEM data source comes from TERRASAR-X with a resolution of 7.5 m.

2.3. Index Formula

2.3.1. Normalized Difference Water Index (NDWI)

Normalized Difference Water Index (NDWI) is a formula in Eq. (1) used in water surface extraction by utilizing the near-infrared (NIR) and green wave bands. (Green) [15].

$$NDWI = \frac{(GREEN - NIR)}{(GREEN + NIR)} \quad (1)$$

The Normalized Difference Water Index is considered an effective index for distinguishing soil and water due to the high absorption of electromagnetic radiation by the water surface, resulting in low reflections [16].

2.3.2. Modified Normalized Difference Water Index (MNDWI)

Modified Normalized Difference Water Index (MNDWI) is the extraction of water surface in residential areas or urban areas [17]. Eq. (2) ANDWI utilizes the green wave (Green) and shortwave infrared 1 (SWIR1).

$$\text{MNDWI} = \frac{(\text{GREEN} - \text{SWIR1})}{(\text{GREEN} + \text{SWIR1})} \quad (2)$$

2.3.3. Augmented Normalized Difference Water Index (ANDWI)

Augmented Normalized Difference Water Index (MNDWI) is a method to extract water surface covered by plants and containing sediments [18]. Eq. (3) ANDWI utilizes blue wave (Blue), green wave (Green), red wave (Red), near-infrared (NIR), shortwave infrared 1 (SWIR1), and shortwave infrared 2 (SWIR2).

$$\text{ANDWI} = \frac{(\text{BLUE} + \text{GREEN} + \text{RED} - \text{NIR} - \text{SWIR1} - \text{SWIR2})}{(\text{BLUE} + \text{GREEN} + \text{RED} + \text{NIR} + \text{SWIR1} + \text{SWIR2})} \quad (3)$$

2.3.4. Soil Adjustment Vegetation Index (SAVI)

Soil Adjustment Vegetation Index (SAVI) is a method used to extract the surface of open land [19]. Eq. (4) SAVI utilizes the red (Red), near-infrared (NIR), and plant density (L).

$$\text{SAVI} = \frac{(\text{NIR} - \text{RED})}{(\text{NIR} + \text{RED} + \text{L})} \times (1 + \text{L}) \quad (4)$$

The value of L, which is the density of plants, ranges from 0 to 1. Thus, the average value of L = 0.5 was used.

2.4. Confusion Matrix

A confusion matrix is a method used to predict algorithms [20]. The algorithm can determine appropriate and inappropriate results, which can be categorized into four possibilities [21]. Table 2 shows four identifications: true positive (TP), true negative (TN), false positive (FP), and false negative (FN).

Table 2 Data confusion matrix

Map	Ground Truth	
	Water	Land
Water	TP	FP
Land	FN	TN

The algorithm can then be measured to obtain validation. The validation results were carried out with image classification using Google Earth images of river borders and bodies. To validate the confusion matrix data, Eq. (5) Accuracy, Eq. (6) Sensitivity, and Eq. (7) Precision are used [22].

$$\text{Accuracy} = \frac{(\text{TP} + \text{TN})}{(\text{TP} + \text{TN} + \text{FP} + \text{FN})} \quad (5)$$

$$\text{Sensitivity} = \frac{\text{TP}}{(\text{TP} + \text{FN})} \quad (6)$$

$$\text{Precision} = \frac{\text{TP}}{(\text{TP} + \text{FP})} \quad (7)$$

2.5. Quasi Unsteady Flow

Hec-Ras can assist in analyzing sediment movement in 2D. Quasi-unsteady flow is used to provide estimates of riverbed changes based on discharge and sediment data. The MPM-Toffaleti method has precise analysis results [23]. The use of the method is effective at a sediment gradation of 0.06 - 0.07 mm.

3. Result and Discussion

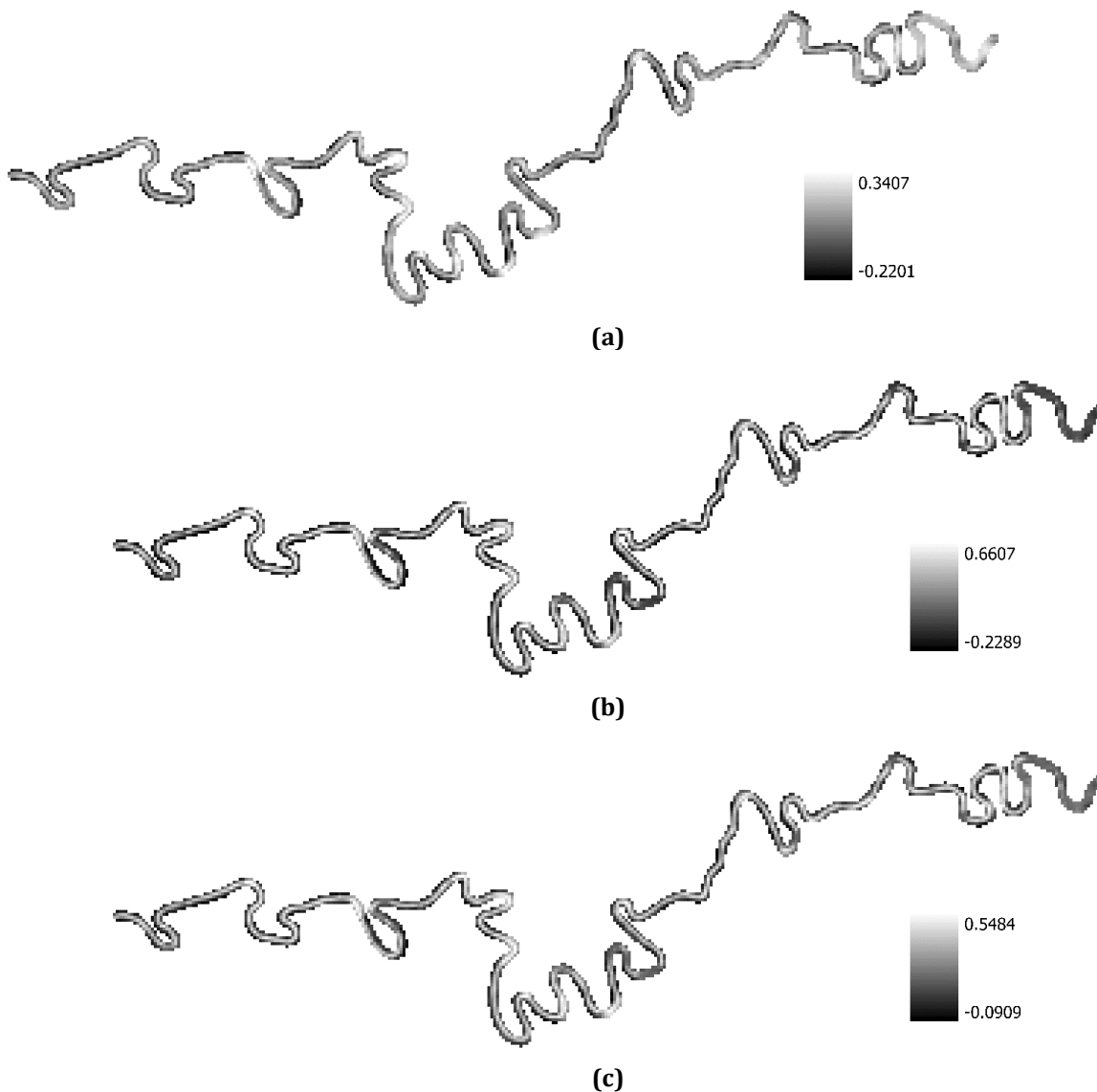
3.1 River Body Extraction

The extracted image of the river flow is obtained from the reflection of the Landsat satellite sensor. The analysis of the four indexes has different river water reflection results. In 2003, Landsat 7 satellites were used (Fig. 3). On

the 2003 Landsat map, many cloud images interfere with the index extraction results (see Fig. 3(a & d)). The NDWI results demonstrate a lack of efficacy in differentiating shadows, clouds, adjacent trees, and open land from the water surface. In comparison to SAVI, it is more proficient in water extractions, demonstrating the capacity to remove open land, although further enhancements are still necessary. MNDWI shows a pretty good extraction process where rivers with mud and narrow streams can be accurately delineated (see Fig. 3(b)). However, the cloud-covered regions remain challenging to extract. Fig. 3(c) shows that ANDWI is an index that can distinguish rivers and other obstructions well, but narrow streams are still a problem.

The extraction of all index rivers in 2013 can be seen in Fig. 4. The river at the time of image capture had a high silt content that could affect the classification. Improving the quality of the satellite image capture should better differentiate the streams (Fig. 4 (d)). The efficiency of SAVI extraction is constrained by the presence of non-natural bands, which impedes the capacity to differentiate between the water surface and vegetation. However, open land and buildings can still be discerned with reasonable accuracy. Meanwhile, Fig. 4(b & c) shows that MNDWI and ANDWI have problems distinguishing river conditions mixed with mud and wet soil used for agricultural land. In this case, MNDWI q the river flow quite clearly. For NDWI extraction, the river image is still quite clear in streams that have high-light reflection, making some parts of the river not fully visible (see Fig. 4(a)).

In 2023, the river extraction results can be seen in Fig 5. The data used comes from Landsat 9 satellites that have more detailed band images. All indexes provide very clear results in distinguishing river flow. However, NDWI and SAVI still have difficulty in differentiating clouds, causing some parts of the river to be lost (Fig. 5(a & d)). MNDWI presents results that almost resemble the original state see Fig. 5(b). ANDWI shows that some impassable streams still have standing water see Fig. 5(c). The development of Landsat satellites has greatly affected the quality of the waves, especially in the NIR and SWIR bands.



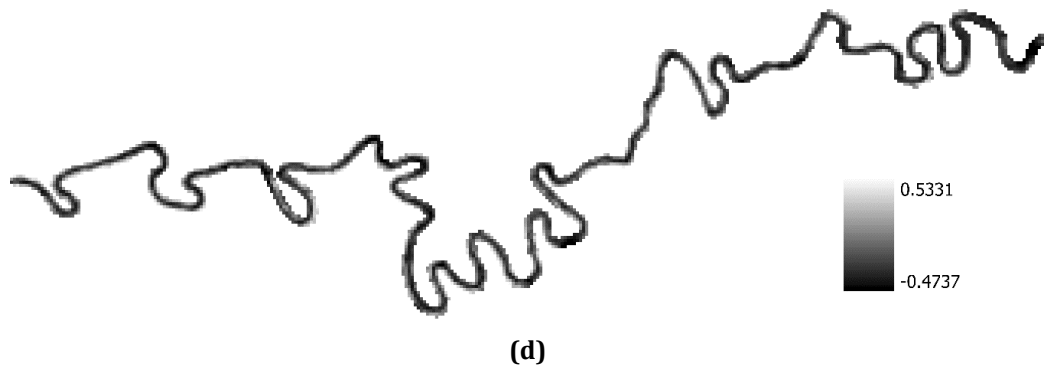
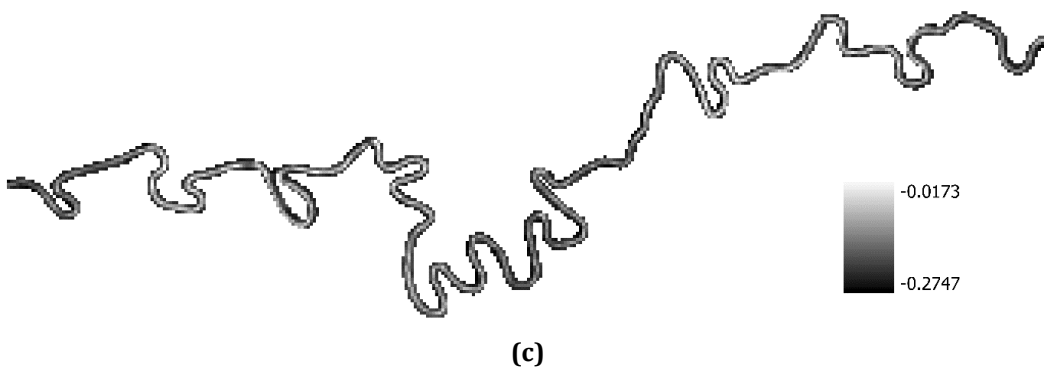
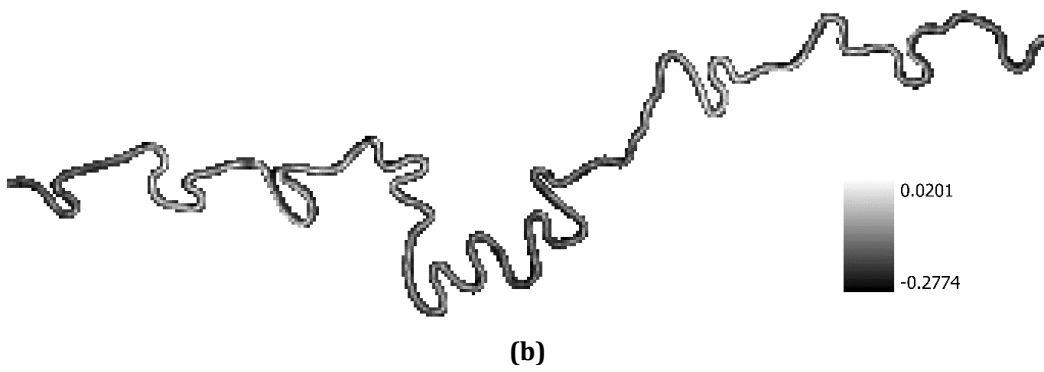
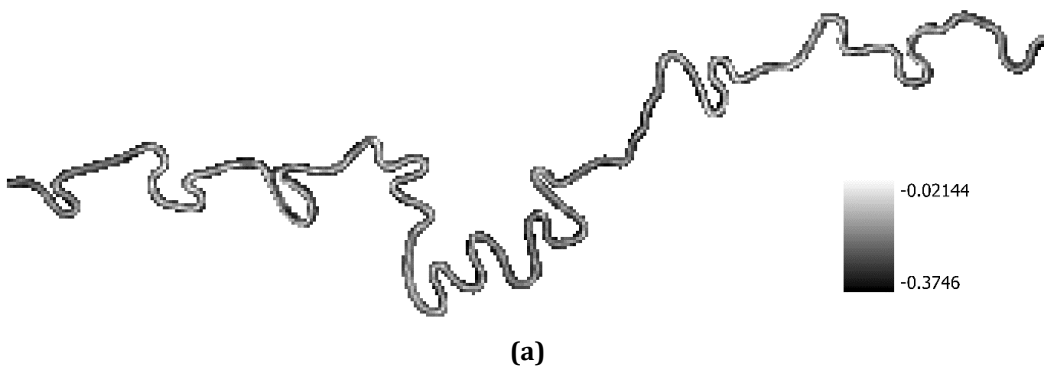


Fig. 3 Extraction river body 2003 (a) NDWI; (b) MNDWI; (c) ANDWI; (d) SAVI



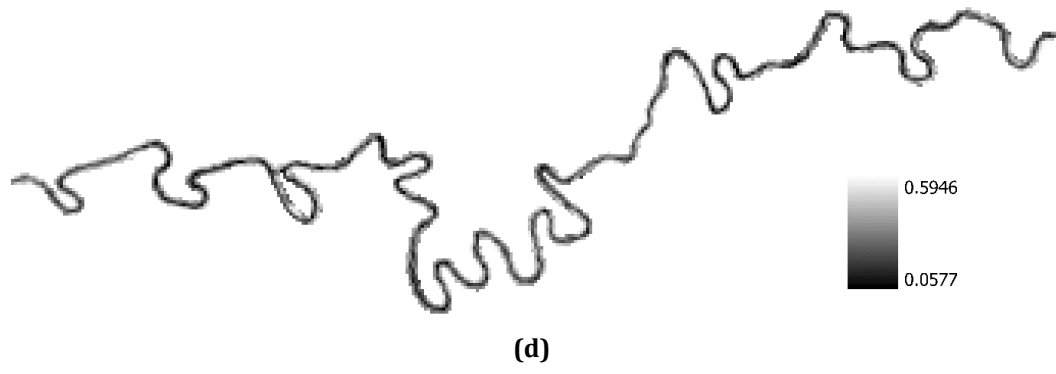
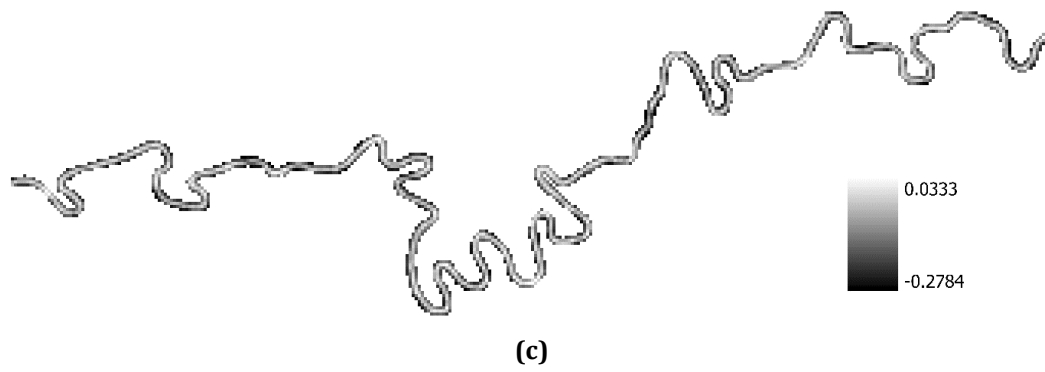
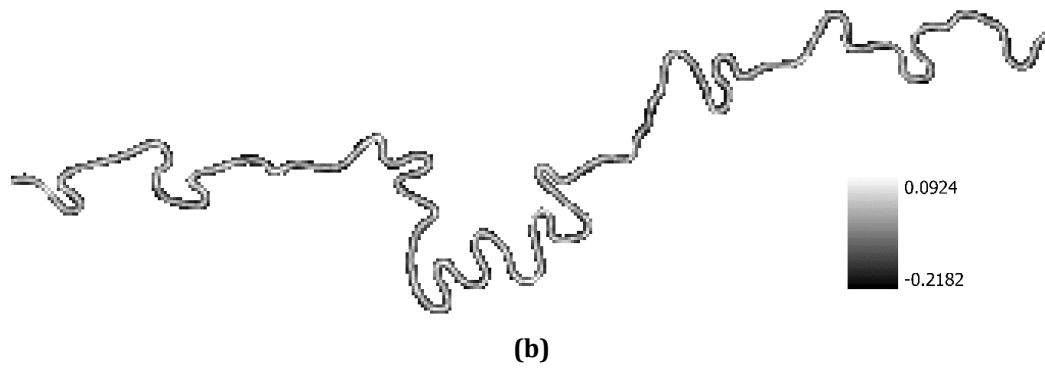
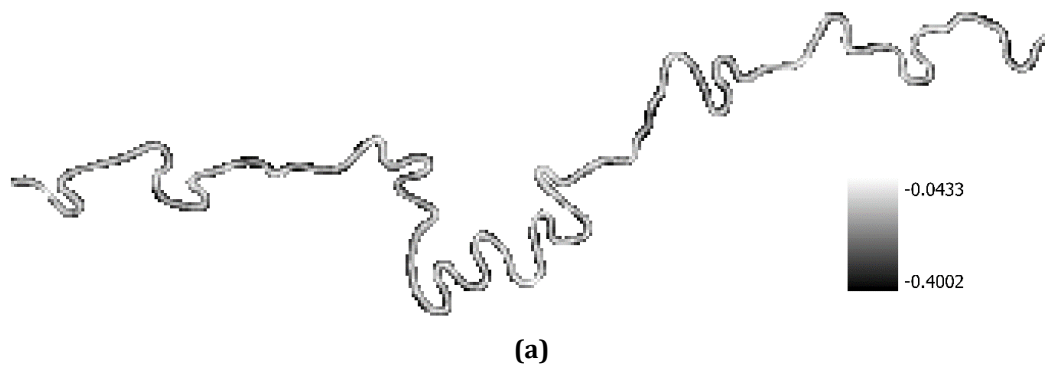


Fig. 4 Extraction river body 2013 (a) NDWI; (b) MNDWI; (c) ANDWI; (d) SAVI



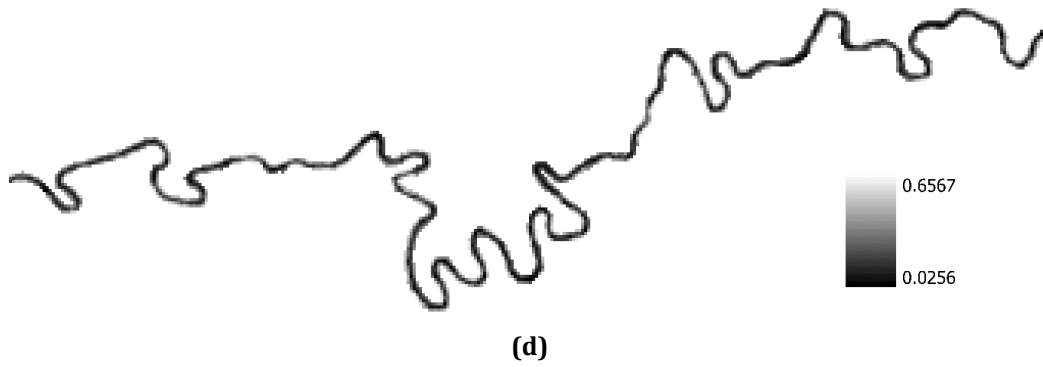


Fig. 5 Extraction river body 2023 (a) NDWI; (b) MNDWI; (c) ANDWI; (d) SAVI

Comparing these indices, Landsat has progressed in image data collection over three years. The level of data resolution in imagery affects classification errors. NDWI has a weakness in distinguishing locations that have shadows and clouds [24]. As seen from the NDWI extension, it is difficult to distinguish water bodies that have low light reflectance. So, in this case, the NIR band greatly affects the NDWI results.

Meanwhile, MNDWI is able to select the shadow part clearly [25]. However, it still causes problems in river sections that have narrow streams with banks. From its development, the SWIR1 band received an improvement in data capture that made it able to distinguish water bodies from other obstructions [26]. In ANDWI, the separation of water bodies is achieved by overcoming obstacles such as clouds, watercolor, shadows, and river width. In this case, the NIR on the shelf also affects the reflection of the water part. SAVI has similar capabilities to NDWI, with clouds and shadows as the main issues. Thus, detecting the flow requires NIR and SWIR 1 data that reflect water [27].

As the flow changes, the sediment transport within the river is also affected, leading to potential changes in river morphology. Manual observing these dynamic changes can be inefficient and laborious. For this reason, remote sensing techniques were used to monitor and analyze these changes. The Lusi River has murky water conditions because it carries a lot of fine material. The stream area is not populated, so there are no obstacles to building detection. Detection problems only exist in vegetation and open land. The NIR sensor that is capable of detecting water bodies [28] is distracted by the riverbank. The problem in detection occurs due to the similar characteristics of the water body with the riverbank, which has sediment and water content. Sloping riverbanks that are not cliffs add to the difficulty in determining the boundary between water and land.

3.2 River area

The index results can show the river flow using time series. The combined results of four indexes, NDWI, ANDWI, MNDWI, and SAVI, show the river flow area. In 2003, the river length was 23.7 km, which was the initial flow length. Then, in 2013, the river flow was reduced to 23.2 km due to the cutting of the river flow upstream (Fig. 6). In 2023, the river flow experienced the same thing to a length of 21.8 km, which occurred in the downstream part of the river.

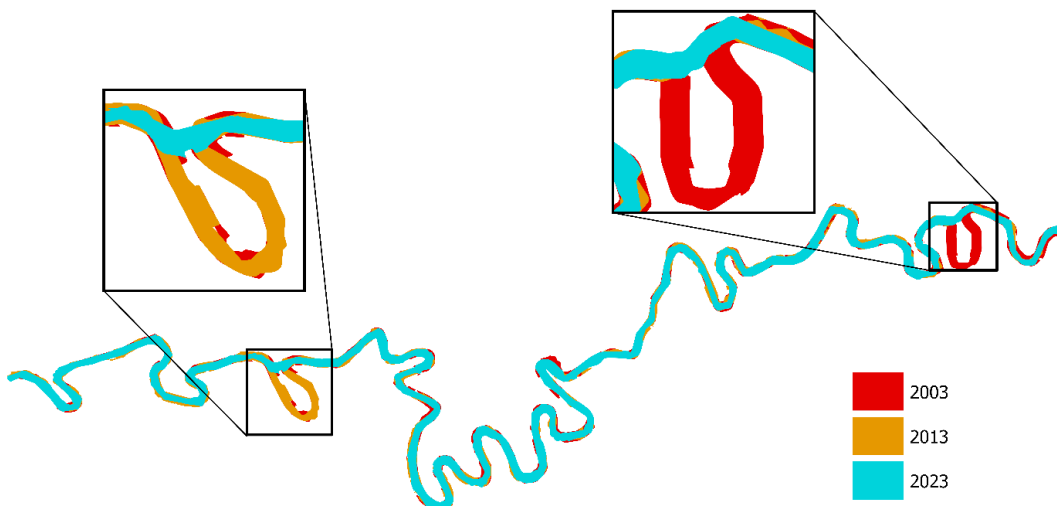


Fig. 6 Water section comparison

The morphology of the Lusi River evolves every year, resulting in changes to the riverbank. For two decades, the river has experienced erosion in its course. Each index has various results when reading the area of the river body. The combined results of river basin separation showed a river area of 1.9352 km² in 2003, 1.7617 km² in 2013, and 1.6406 km² in 2023. The reduction in the river area of 0.12 ± 0.17 km² is the result of the combination of all indexes, which is in the form of displacement of bends and cutting of river flow. Erosion that occurred from 2003 to 2013 amounted to 0.1942 km² and from 2013 to 2023 amounted to 0.1177 km², indicating a decrease in sediment movement activity in the river. Of all, the SAVI index shows a high average erosion of 0.29 ± 0.48 km². MNDWI shows the ability to maintain the river body at 1.27 ± 1.36 km².

Table 3 Surface area river

Index	Area (km ²)			Unchanged (km ²)		Erosion (km ²)	
	2003	2013	2023	2013	2023	2013	2023
NDWI	1.5163	0.8798	1.2460	0.7597	0.7706	0.1201	0.4755
MNDWI	1.7918	1.5708	1.4406	1.3634	1.2704	0.2074	0.1702
ANDWI	1.4466	1.3844	1.4841	1.1087	1.2422	0.2756	0.2418
SAVI	1.1680	1.0200	1.3994	0.7300	0.9211	0.2900	0.4783
Combine	1.9352	1.7617	1.6406	1.5673	1.5230	0.1943	0.1177

As a result, using indexes from the Landsat 7 SAVI platform gave great results with consistent values of accuracy, precision, and sensitivity. However, the following year, there was a considerable decline in performance. Landsat-8 data improved the NDWI, ANDWI, and MNDWI index results from before. ANDWI on Landsat-8 provides quite accurate water body detection results, seen from the high accuracy, precision, and sensitivity values, which are almost the same as MNDWI. Analysis using Landsat-9 showed that almost all indices gave satisfactory results compared to Landsat 7 and 8 [29], indicated by the percentage of data accuracy with a value of >80 percent, with the best performance obtained by ANDWI followed by NDWI.

The Lusi River experienced a reduction in flow length every 10 years. During that time, the Lusi River also experienced a decrease in river width. The erosion that occurs is quite high due to the large amount of discharge that flows. The stream is located in a farming and open land area that is not included in the urban area. This condition is also a factor in flow changes due to the absence of human influence because no problems occur due to large erosion.

Cutoff of the Lusi River flow occurred twice at sharp turns. In addition, the cutoff is located in the upstream and downstream streams that are already close together. The minimum distance between the outermost cliffs of the stream is about 100 m to cut off the flow. These conditions are also supported by the straight flow that comes with great energy [30]. The view in Fig. 7 shows three locations where a cutoff is likely to occur. These locations were chosen because of their similar characteristics to previous cutoffs.

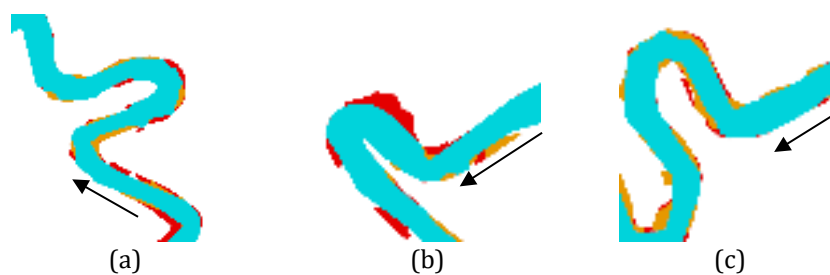


Fig. 7 Indication of where the cutoff occurred: (a) Location 1; (b) Location 2; (c) Location 3

3.3 Accuracy Data

Based on the results of the extraction of the water body, the Lusi River has a flow cut. This condition affects the accuracy of the points to get index conformity with the original situation. Each point in each stream is given 200 m starting from the upstream (Fig. 8) to reduce errors in the analysis. Ground truth data was obtained from Google Earth at the same time as the extraction. However, data validation was required to get the index to match the image. An evaluation was used to categorize water and land (soil, vegetation, buildings). In 2003, a total of 118 points along the stream were obtained. MNDWI obtained the highest water body correction rate with 55 points, which gave it the highest sensitivity value of 0.98 percent. Still, the value was directly proportional to the data error (see Table 4). MNDWI gets an accuracy value of 0.69 percent and a precision of 0.60 percent, which is the lowest result. SAVI results show index consistency with an accuracy of 0.80 percent, precision of 0.74 percent, and

sensitivity of 0.83 percent. However, SAVI will focus on processing images with soil data division and still distinguish water bodies. For a decade, the Lusi River experienced a reduction in flow, so in 2013, a total of 115 points were obtained. This year, ANDWI became an index with a high accuracy value of 0.84 percent and a precision of 0.80 percent. High NIR data from Landsat 8 played a major role in the values obtained. SAVI still shows consistency in detecting land. MNDWI has obstacles in distinguishing water bodies from land, as evidenced by the low accuracy and precision values. However, the highest sensitivity value is obtained by MNDWI with 0.98 percent.

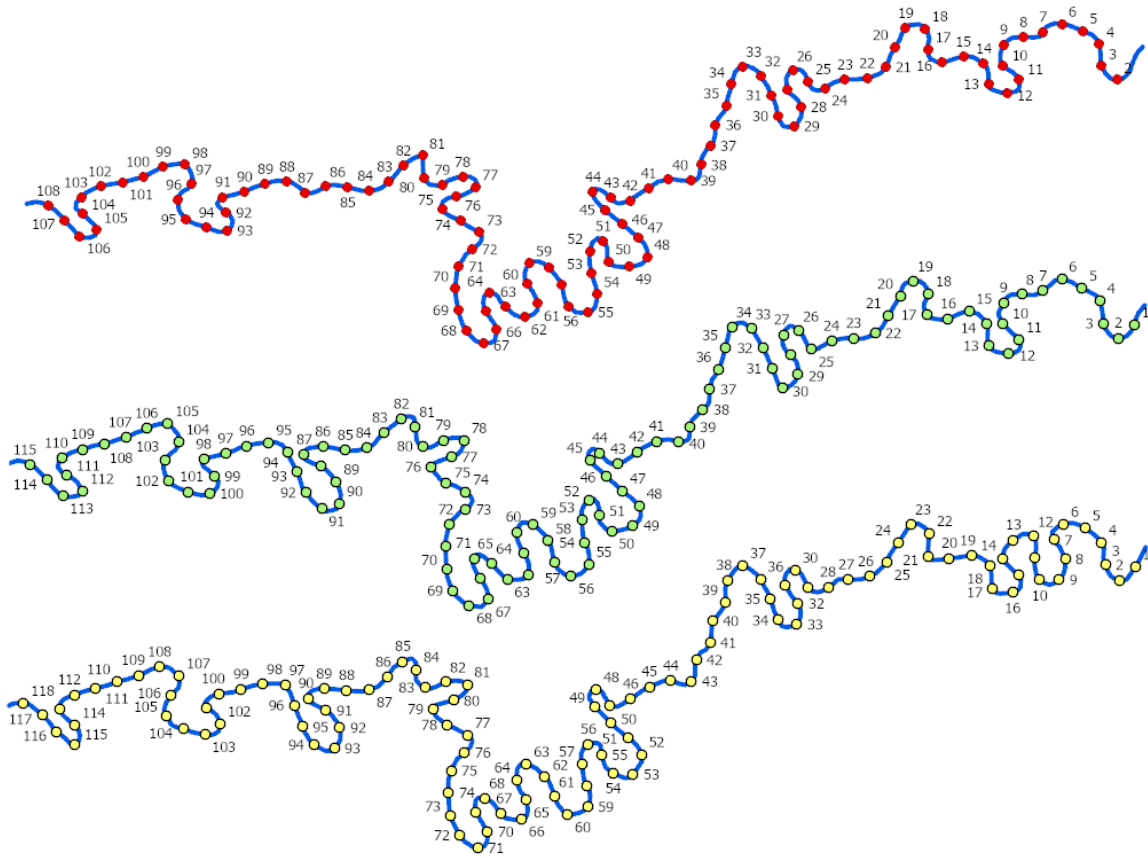


Fig. 8 Point ground truth 2003-2023

Table 4 Result confusion matrix

Year	Index	Result				Accuracy (%)	Sensitifity (%)	Precision (%)
		TP	FP	FN	TN			
2003	NDWI	49	26	6	37	0.73	0.89	0.65
	MNDWI	55	36	1	26	0.69	0.98	0.60
	ANDWI	47	25	9	37	0.71	0.84	0.65
	SAVI	43	15	9	51	0.80	0.83	0.74
2013	NDWI	54	19	8	40	0.77	0.87	0.74
	MNDWI	53	36	1	34	0.68	0.98	0.60
	ANDWI	57	14	3	25	0.85	0.95	0.80
	SAVI	47	23	5	41	0.76	0.90	0.67
2023	NDWI	56	12	1	38	0.88	0.98	0.82
	MNDWI	54	11	7	35	0.83	0.89	0.83
	ANDWI	63	5	4	35	0.92	0.94	0.93
	SAVI	52	18	3	34	0.80	0.95	0.74

As a result, in 2003, the SAVI platform gave satisfactory results with consistent accuracy, precision, and sensitivity values. But the following year saw a considerable decline in performance. Landsat-8 data in 2013 improved the results of all indexes. ANDWI this year provides fairly accurate water body detection results, as seen from the high accuracy, precision, and sensitivity values similar to MNDWI. In 2023, using Landsat-9, almost all indices gave satisfactory results, indicated by the percentage of data accuracy with a value of > 80 percent, with the best performance obtained by ANDWI followed by NDWI.

3.4 Sediment Movement

Sediment analysis with Hec-RAS was performed for two time periods. All simulations were conducted for one year to maximize the potential for sediment movement. Possession discharge data were not recorded until 2022, so the data used was one year prior to the monitoring period. The first simulation period was conducted to monitor sediment movement in 2013 using cross-data from direct measurements and discharge data from January to December 2012. In the second simulation period, to determine sediment movement in 2023, DEM data were used with discharge data from January to December 2022. The simulations were performed by ignoring the presence of other sediment material factors (waste, log) to show the same performance in the comparison of results. The logic of sediment movement and erosion uses the Toffaleti-MPM formula combined to optimize the simulation of fine grain size.

Simulation indicated that the riverbed exhibited changes in 2013, with a range of -1.1 ± 2.03 m (Fig. 9). The slope value obtained is 0.00038. It was then known that 32.4 percent of the flow experienced aggradation, 64 percent experienced erosion, and 3.6 percent of the flow had no change. The river flow is cut at points 6-12 (1200 - 2400 m), which can be seen to experience riverbed erosion, although not high. In 2023, the flow slope value is 0.00035 (Fig. 10). With this value, the range of changes in the riverbed is -2.69 ± 1.29 m. Hence, the aggradation is 27 percent, riverbed erosion is 70.4 percent, and as much as 2.6 percent of the riverbed has not changed. These results show that erosion of the riverbed continues to increase every year. This event is caused by an increase in discharge, which affects the movement of sediment in the river flow.

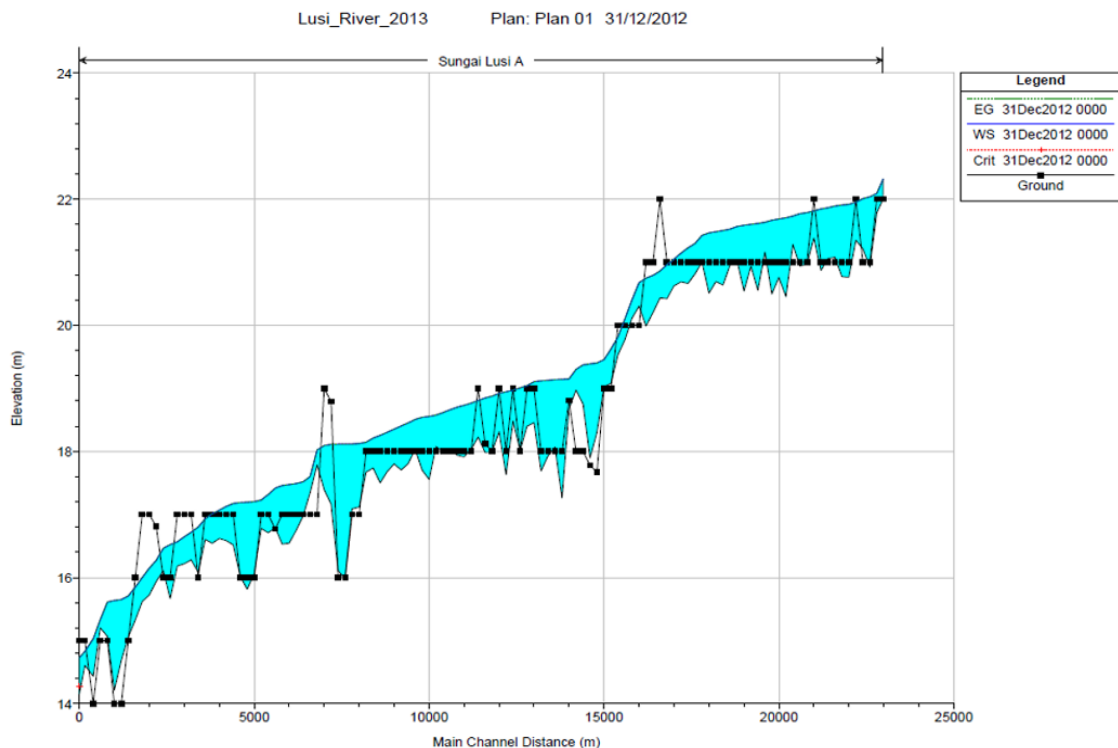


Fig. 9 Plot profile river 2013

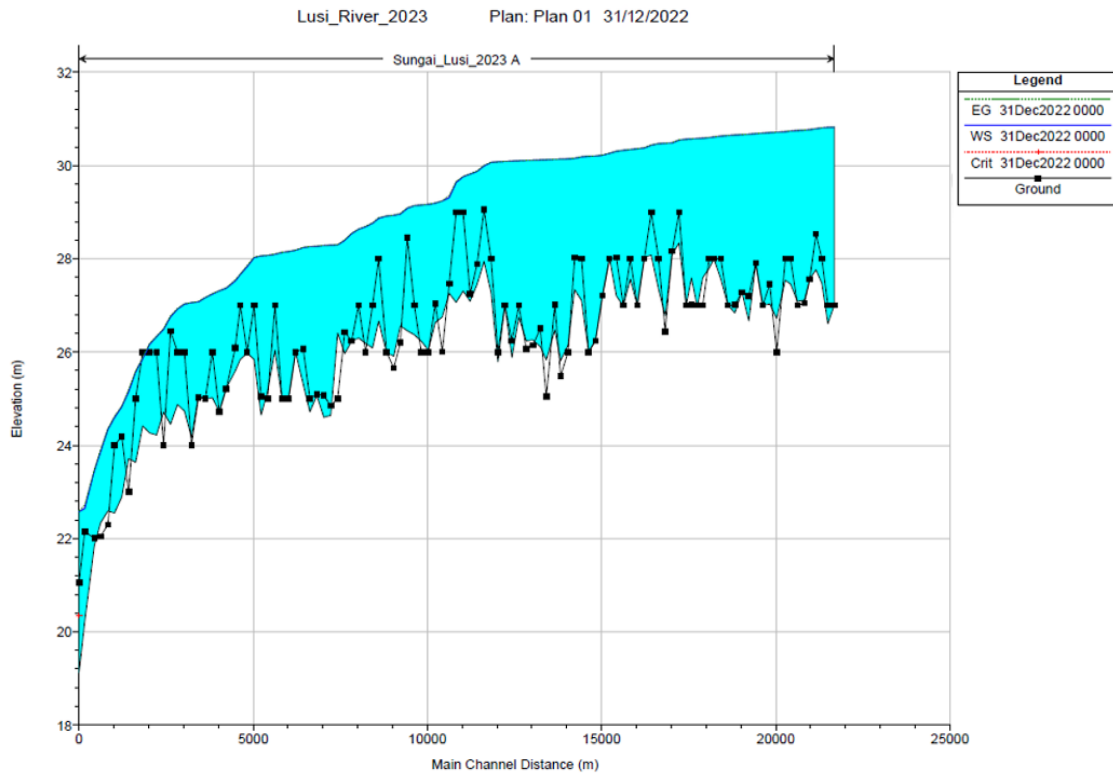


Fig. 10 Plot profile river 2023

In modeling, roughness and geometry parameters greatly affect the prediction results [31]. Simulations using direct measurement data and DEMs produce different results. The lowest elevation should not have a considerable change in elevation. Java Island suffers from land subsidence every year [32]. So, the elevation comparison between manual and automatic measurements has a difference. In this analysis, elevation accuracy is lacking in the simulation.

The simulation of riverbed erosion in 2023 shows a higher erosion rate than in 2013. A high increase in discharge in a decade has a significant impact. However, when compared with the data from the Remote Sensing analysis, the width of the water body is not proportional to the level of riverbed erosion that occurs.

4. Conclusion

NDWI, MNDWI, ANDWI, and SAVI can generally identify river bodies with high mud content. Although in some parts, it is still difficult to distinguish it from river cliffs. Sensor upgrades from Landsat 7 to Landsat 9 have provided good data quality. The Lusi River has had one cutoff phenomenon in a decade, so in two decades, there have been two phenomena. The cutoffs in the Lusi River have some similar characteristics. By looking at these characteristics, we can see three other locations where flow cutoffs are likely to occur. The riverbank erosion results obtained from all indexes were validated by simulating riverbed erosion. The level of erosion on the river bank and riverbed does not have a quite tangent correlation because each result has a different erosion rate.

Acknowledgement

This research was conducted using the facilities of the Master's Program in Civil Engineering, Postgraduate Program at Universitas Muhammadiyah Yogyakarta, Indonesia. A special acknowledgment is given to PT. Esri Indonesia from providing the ArcGIS Pro software license for UMY.

Conflict of Interest

The authors declare that there is no conflict of interest regarding the publication of the paper.

Author Contribution

The authors confirm their contribution to the paper as follows: Draft manuscript preparation, analysis of remote sensing, modeling, and simulation Hec-RAS, representation data: Diva Darma Wijaya. Research plan, supervision the project, literature review: Nursetiawan; Analysis of river morphology, revision of manuscript paper: Jazaul Ikhsan. All authors reviewed the results and approved the final version of the manuscript.

References

- [1] Xue, Y., Qin, C., Wu, B., Zhang, G., Fu, X., Ma, H., Li, D. & Wang, B. (2023) Simulation of runoff process based on the 3-D river network, *Journal of Hydrology*, 626(Part A), 130192, <https://doi.org/10.1016/j.jhydrol.2023.130192>
- [2] Freeman, J., Robinson, E., Beckman, N. G., Bird, D., Baggio, J. A. & Anderies, J. M. (2020) The global ecology of human population density and interpreting changes in paleo-population density, *Journal of Archaeological Science*, 120, 105168, <https://doi.org/10.1016/j.jas.2020.105168>
- [3] Xiao, Y., Liu, J., Gualtieri, C., Fu, J., Gu, R., Wang, Z., Zhang, T. & Zhou, J. (2022) The effect of natural and engineered hydraulic conditions on river-floodplain connectivity using hydrodynamic modeling and particle tracking analysis, *Journal of Hydrology*, 615(Part A), 128578, <https://doi.org/10.1016/j.jhydrol.2022.128578>
- [4] Kusena, W., Chemura, A., Dube, T., Nicolau, M. D. & Marambanyika, T. (2022) Landuse and landcover change assessment in the Upper Runde sub-catchment, Zimbabwe and possible impacts on reservoir sedimentation, *Physics and Chemistry of the Earth, Parts A/B/C*, 126, 103105, <https://doi.org/10.1016/j.pce.2021.103105>
- [5] Li, Z., Yan, C. & Boota, M. W. (2022) Review and outlook of river morphology expression, *Journal of Water and Climate Change*, 13(4), 1725-1747, <https://doi.org/10.2166/wcc.2022.449>
- [6] Namara, W. G., Damisse, T. A. & Tufa, F. G. (2022) Application of HEC-RAS and HEC-GeoRAS model for flood inundation mapping, the case of Awash bello flood plain, upper Awash River Basin, oromiya regional state, Ethiopia, *Modeling Earth Systems and Environment*, 8(2), 1449-1460, <https://doi.org/10.1007/s40808-021-01166-9>
- [7] Ai, L., Walter, T. R., Aguilera, F., Layana, S., Mania, R., Kujawa, C., Zimmer, M. & Inostroza, M. (2023) Crater morphology, nested ring structures, and temperature anomalies studied by unoccupied aircraft system data at Lascar volcano, northern Chile, *Journal of Volcanology and Geothermal Research*, 439, 107840, <https://doi.org/10.1016/j.jvolgeores.2023.107840>
- [8] Paramita, B. & Matzarakis, A. (2023). Urban Biometeorology of Tropical Climate: Af, Am, Aw, a Propensity of 34 Provincial Cities in Indonesia. In *Climate Change and Cooling Cities* (pp. 283-296). Springer. https://doi.org/https://doi.org/10.1007/978-981-99-3675-5_16
- [9] Hemmeler, S., Marra, W., Markies, H. & De Jong, S. M. (2018) Monitoring river morphology & bank erosion using UAV imagery—A case study of the river Buëch, Hautes-Alpes, France, *International Journal of Applied Earth Observation and Geoinformation*, 73, 428-437, <https://doi.org/10.1016/j.jag.2018.07.016>
- [10] Hinton, J. (1996) GIS and remote sensing integration for environmental applications, *International Journal of Geographical Information Systems*, 10(7), 877-890, <https://doi.org/10.1080/02693799608902114>
- [11] Parelus, E. J. (2023). A Review of Deep-Learning Methods for Change Detection in Multispectral Remote Sensing Images. *Remote Sensing*, 15(8), 2092, <https://doi.org/10.3390/rs15082092>
- [12] Fang-fang, Z., Bing, Z., Jun-sheng, L., Qian, S., Yuanfeng, W. & Yang, S. (2011) Comparative analysis of automatic water identification method based on multispectral remote sensing, *Procedia Environmental Sciences*, 11, 1482-1487, <https://doi.org/10.1016/j.proenv.2011.12.223>
- [13] Duguma, T. A. (2023) RS and GIS analysis of the groundwater potential zones in the Upper Blue Nile River Basin, Ethiopia, *Journal of Hydrology: Regional Studies*, 46, 101344, <https://doi.org/10.1016/j.ejrh.2023.101344>
- [14] Gayo, A. A. P., Zainabun, Z. & Arabia, T. (2022). Karakterisasi Morfologi dan Klasifikasi Tanah Aluvial Menurut Sistem Soil Taxonomy di Kabupaten Aceh Besar, *Jurnal Ilmiah Mahasiswa Pertanian*, 7(3), 503-508, <https://doi.org/10.17969/jimfp.v7i3.20885>
- [15] Gao, B.-C. (1996). NDWI—A normalized difference water index for remote sensing of vegetation liquid water from space, *Remote sensing of environment*, 58(3), 257-266, [https://doi.org/10.1016/S0034-4257\(96\)00067-3](https://doi.org/10.1016/S0034-4257(96)00067-3)
- [16] Laonamsai, J., Julphunthong, P., Saprathet, T., Kimmany, B., Ganchanasuragit, T., Chomcheawchan, P. & Tomun, N. (2023) Utilizing NDWI, MNDWI, SAVI, WRI, and AWEI for Estimating Erosion and Deposition in Ping River in Thailand, *Hydrology*, 10(3), 70, <https://doi.org/10.3390/hydrology10030070>
- [17] Xu, H. (2006). Modification of normalised difference water index (NDWI) to enhance open water features in remotely sensed imagery, *International journal of remote sensing*, 27(14), 3025-3033. <https://doi.org/10.1080/01431160600589179>
- [18] Rad, A. M., Kreitler, J. & Sadegh, M. (2021) Augmented Normalized Difference Water Index for improved surface water monitoring, *Environmental Modelling & Software*, 140, 105030. <https://doi.org/10.1016/j.envsoft.2021.105030>
- [19] Huete, A. R. (1988). A soil-adjusted vegetation index (SAVI), *Remote sensing of environment*, 25(3), 295-309. [https://doi.org/10.1016/0034-4257\(88\)90106-X](https://doi.org/10.1016/0034-4257(88)90106-X)

- [20] Ruuska, S., Hämäläinen, W., Kajava, S., Mughal, M., Matilainen, P. & Mononen, J. (2018). Evaluation of the confusion matrix method in the validation of an automated system for measuring feeding behaviour of cattle, *Behavioural processes*, 148, 56-62, <https://doi.org/10.1016/j.beproc.2018.01.004>
- [21] Luque, A., Carrasco, A., Martín, A. & de Las Heras, A. (2019) The impact of class imbalance in classification performance metrics based on the binary confusion matrix, *Pattern Recognition*, 91, 216-231, <https://doi.org/10.1016/j.patcog.2019.02.023>
- [22] Valero-Carreras, D., Alcaraz, J. & Landete, M. (2023) Comparing two SVM models through different metrics based on the confusion matrix, *Computers & Operations Research*, 152, 106131, <https://doi.org/10.1016/j.cor.2022.106131>
- [23] Szalkiewicz, E., Dysarz, T., Kałuża, T., Malinger, A. & Radecki-Pawlik, A. (2019) Analysis of in-stream restoration structures impact on hydraulic condition and sedimentation in the Flinta River, Poland, *Carpathian Journal of Earth and Environmental Sciences*, 14(2), 275-286, <https://doi.org/10.26471/cjees/2019/014/079>
- [24] Chisadza, B., Gwate, O., Ncube, F., Moyo, N. & Chiwara, P. (2022), Detecting land surface water changes in the Upper Mzingwane sub-catchment using remotely sensed data, *Aqua Water Infrastructure, Ecosystems, and Society*, 71(10), 1180-1196, <https://doi.org/10.2166/aqua.2022.089>
- [25] Pereira, L. E., Lo, E. L. & Paranhos Filho, A. C. (2022) Analysis of the Taquari Megafan through radiometric indices, *Journal of South American Earth Sciences*, 119, 104034, <https://doi.org/10.1016/j.jsames.2022.104034>
- [26] Hadibasyir, H. Z., Firdaus, N. S., Fikriyah, V. N. & Sari, D. N. (2023) Assessing performance of modified spectral indices as land surface temperature indicators in tropical urban areas. IOP Conference Series: Earth and Environmental Science, 1190, 012005, <https://doi.org/10.1088/1755-1315/1190/1/012005>
- [27] Chen, F., Chen, X., Van de Voorde, T., Roberts, D., Jiang, H. & Xu, W. (2020) Open water detection in urban environments using high spatial resolution remote sensing imagery, *Remote Sensing of Environment*, 242, 111706, <https://doi.org/10.1016/j.rse.2020.111706>
- [28] Khalifeh Soltanian, F., Abbasi, M. & Riyahi Bakhtyari, H. R. (2019) Flood monitoring using NDWI and MNDWI spectral indices: A case study of Aghqala flood-2019, Golestan Province, Iran, *International Archives of the Photogrammetry, Remote Sensing and Spatial Information Sciences*, XLII-4/W18, 605-607, <https://doi.org/10.5194/isprs-archives-XLII-4-W18-605-2019>
- [29] Chen, J., Wang, Y., Wang, J., Zhang, Y., Xu, Y., Yang, O., Zhang, R., Wang, J., Wang, Z., Lu, F. & Hu, Z. (2024) The Performance of Landsat-8 and Landsat-9 Data for Water Body Extraction Based on Various Water Indices: A Comparative Analysis, *Remote Sensing*, 16(11), 1984, <https://doi.org/10.3390/rs16111984>
- [30] Wu, X., Hu, X. & Zhang, X. (2023) Experimental Study on Neck Cutoff in Meandering River under Variable Discharges, *Water (Switzerland)*, 15(5), 841, <https://doi.org/10.3390/w15050841>
- [31] Pappenberger, F., Beven, K., Horritt, M. & Blazkova, S. (2005) Uncertainty in the calibration of effective roughness parameters in HEC-RAS using inundation and downstream level observations, *Journal of Hydrology*, 302(1-4), 46-69. <https://doi.org/10.1016/j.jhydrol.2004.06.036>
- [32] Ramadhanty, N. A. & Yusuf, R. (2024) The influence of groundwater use on land subsidence in Bandung City. IOP Conference Series: Earth and Environmental Science, 1311, 012066, <https://doi.org/10.1088/1755-1315/1311/1/012066>